ELSEVIER

Chemical Engineering Journal 100 (2004) 11–22

Chemical Engineering Journal

www.elsevier.com/locate/cej

Improved kinetics-based gold cyanide extraction with mixture of LIX79 + TOPO utilizing hollow fiber membrane contactors

Anil Kumar Pabby[1], R. Haddad, F.J. Alguacil, A.M. Sastre*

Department of Chemical Engineering, Universitat Politècnica de Catalunya, ETSEIB, Av. Diagonal 647, E-8028 Barcelona, Spain

Received 21 January 2003; accepted 14 November 2003

Abstract

Dispersion-free solvent extraction of gold(I) ($Au(CN)_2^-$) from alkaline cyanide media was performed using porous hydrophobic hollow fibers with mixtures of membrane extractants. The organic extractant used for gold(I) extraction was LIX79 (*N*,*N*′-bis(2-ethylhexyl)guanidine) alone and a mixture of trioctylphosphine oxide (TOPO) + LIX79 diluted with *n*-heptane. The mixture of LIX79 + TOPO affords a better performance than LIX79 alone. It took 300 s to extract more than 95% gold with equimolar LIX79 + TOPO (0.125 M), whereas pure LIX79 (0.375 M) took 1860 s to reach the same percentage level of gold extraction (over six times slower). The mass transfer coefficient's (K_{Au}^{E}) value was around four times higher with the equimolar mixture of 0.125 M LIX79 + 0.125 M TOPO than with LIX79/*n*-heptane alone. Extraction of $Au(CN)_2^-$ from alkaline cyanide solutions with TOPO alone was also observed, indicating that gold(I) complexation takes place probably by a solvation reaction mechanism ($M^+ \cdots Au(CN)_2 \cdot S_n$). A model is presented which describes the extraction mechanism, indicating different rate-controlling steps. The validity of this model was evaluated with experimental data and was found to tie in well with theoretical values.

Keywords: The Dispersion-free membrane extraction; Trioctylphosphine oxide (TOPO); *N*,*N*-bis(2-ethylhexyl)guanidine (LIX79)

1. Introduction

Gold recovery from various cyanide solutions is achieved in the gold mining industry by employing a commercial process which is based on the initial leaching of ores with cyanide solutions combined with a step consisting in gold cyanide adsorption with activated carbon. A lack of selectivity is found while using activated carbon in the presence of mixtures of other metal cyanides [1]. Therefore, in recent years, research efforts have been made to replace activated carbon with other alternative techniques that are capable of overcoming these difficulties. In this direction, membrane extraction processes using porous hollow fibers are of particular interest because of their versatility and the fact that they overcome problems encountered in the conventional gold process using activated carbon. Dispersion-free membrane extraction (DFMEX) is simply a liquid–liquid extraction in a hollow fiber contactor in which aqueous and organic streams flow through the capillary shell side and come into contact at the pore mouth without dispersion, which minimizes the possibility of emulsion/third phase or crud formation with the extractant. The viability, advantages, disadvantages and potential of this technique are already described in detail in our recently published chapter [2] and by Gableman and Hwang in their comprehensive review on hollow fiber contactors [3]. In addition, application-oriented studies for gold recovery from hydrometallurgical alkaline solutions were carried out by our research group, with LIX79 (*N*,*N*′-bis(2-ethylhexyl)guanidine) dissolved in *n*-heptane system using the integrated membrane process (IMP) with two modules (more details of this process are provided in Section 2) [4] and in batch mode using one module (extraction and stripping separately) (more details of IMP and batch process are provided in Section 2) [5]. Furthermore, studies conducted with LIX79 alone resulted in poor selectivity towards cyanide salts of zinc and silver [6–8]. As suggested by Mooiman and Miller [9–11], the addition of organophosphorous compounds such as tri-*n*-butylphosphate (TBP), trioctylphosphine oxide (TOPO) or dibutylphosphate (DBP) to LIX79 can improve the amine-based system for the extraction of gold cyanide solution. Therefore, the hollow fiber-supported liquid membrane configuration was checked

* Corresponding author. Tel.: +34-93-401-6557; fax: +34-93-401-6600.
E-mail addresses: dranil@bom3.vsnl.net.in (A.K. Pabby), ana.maria.sastre@upc.es (A.M. Sastre).
[1] On leave from PREFRE, Nuclear Recycle Group, Bhabha Atomic Research Centre, Tarapur 401502, India. Fax: +91-2525-282158.

1385-8947/$ – see front matter © 2003 Published by Elsevier B.V.
doi:10.1016/j.cej.2003.11.014

Nomenclature

C	metal concentration (g/cm^3)
d	diameter of one fiber (cm)
d_i	inner fiber diameter
d_{lm}	logarithmic mean diameter of one fiber
d_o	outer fiber diameter
D_h	hydraulic diameter (cm)
D_m	diffusion coefficient of metal complex in membrane
D_s	diffusion coefficient of solute on shell side
D_t	diffusion coefficient of solute on tube side (cm^2/s)
H	partition coefficient of extraction and stripping
k_e	mass transfer coefficient of organic (cm/s)
k_f	mass transfer coefficient of aqueous feed (cm/s)
k_i	rate of interfacial reaction at surface (cm/s)
k_m	membrane mass transfer coefficient (cm/s)
k_s	organic mass transfer coefficient (cm/s)
k_{st}	mass transfer coefficient for stripping (cm/s)
K_{ex}	extraction constant
K^E_{Au}, K^S_{Au}	overall mass transfer coefficients for extraction and stripping, respectively (cm/s)
L	fiber length (cm)
N_{Gz}	Graetz number ($N_{Gz} = d^2\upsilon/DL$)
N_{Re}	Reynolds number for feed ($N_{Re} = \upsilon d/\eta$)
N_{Sc}	Schmidt number ($N_{Sc} = \eta/D$)
N_{Sh}	Sherwood number for tube side ($N_{Sh} = k_f d_i/D_t$) and shell side ($N_{Sh} = k_s D_h/D_s$)
Q	flow rate (cm^3/s)
r	hollow fiber radius (cm)
r_{lm}	logarithmic mean radius of lumen (cm)
$[R_{org}]$	concentration of organic extractant (LIX79)
R^0_m, R^0_f, R^0_s, R^0_i, R^0_{st}	fractional resistance due to membrane, feed, solvent, interfacial reaction and stripping, respectively
R_m, R_f, R_s, R_i, R_{st}	resistance due to membrane, feed, solvent, interfacial reaction and stripping, respectively (S/cm)
$[S_{org}]$	concentration of organic extractant (TOPO)
t_m	thickness of the fiber membrane (cm)
V_e	volume of organic tank (cm^3)
V_f	volume of feed tank (cm^3)
V_m	volume of hollow fibers (cm^3)
V_s	volume of stripping tank (cm^3)

Greek letters

β	shell side constant
ε	porosity
η_s	viscosity of organic solution (cP or g/cm s)
η_t	viscosity of aqueous feed/stripping solution (cP or g/cm s)
τ	tortuosity of the membrane
υ_f or υ_t	velocity of liquid on fiber side (cm/s)
υ_s	velocity of liquid on shell side (cm/s)
ϕ	packing fraction of HF module

Superscript

0	refers to the concentration at time zero

Subscripts

e/s	for extract/strip
f	feed
i	for inner radii
m	membrane
o	for outer radii
s	strip side or shell side
t	tube side

with Au(I) from alkaline cyanide media using a mixture of LIX79+TOPO as extractant [12]. Although the results were consistent with the operating conditions and stability of the system, high flow rates (to obtain high mass transfer) could not be used due to the impregnation mode, which could force the organic extractant out of the pore. Therefore, to obtain a high mass transfer coefficient, the dispersion-free solvent extraction (DFSX) mode was selected. The main objective of carrying out this study is to improve the kinetics of the whole system by employing LIX79 + TOPO as extractant and to obtain a consistent and stable performance under the experimental conditions studied. The results obtained with the LIX79 + TOPO and LIX79 alone are compared in order to justify the improvement in the system. The overall mass transfer coefficients for extraction (K^E_{Au}) and stripping (K^S_{Au}) of Au(I) were calculated. The separation and recovery of gold in the presence of other metal cyanide salts of Fe(II), Cu(I), Ni(II), Ag(I) and Zn(II) from alkaline cyanide solutions using LIX79 + TOPO/*n*-heptane is described in our earlier publication dealing with HF-SLM mode [12]. In addition, the selectivity of Au(I) with respect to Zn(II) and Ag(I) cyanide salts was found to be improved [12]. A model is presented which describes the extraction mechanism, indicating different rate-controlling steps.

2. Experimental procedure

2.1. Reagents

A stock solution of Au(I) (5 g/l) was prepared from pure solid $KAu(CN)_2$ (Johnson Mattey Chemicals, Karlsruhe, Germany) dissolved in NaCN (Merck). The organic solvent

Table 1
Details of contactors and hollow fiber membrane

(a) Details of contactors	
Type of module	5PCG-259 (contactor)
Number of fibers	10000
Module diameters (cm)	8
Module length (cm)	28
Active interfacial area (m^2)	1.4
(b) Details of hollow fiber membrane	
Fiber i.d. (cm)	24.0×10^{-3}
Fiber o.d. (cm)	30.0×10^{-3}
Fiber wall thickness (cm)	3.0×10^{-3}
Fiber length (cm)	15
Porosity (%)	30
Pore size (μm)	0.03
Polymeric material	Polypropylene
Hydraulic diameter (cm)	0.1
Area per unit volume (cm^2/cm^3)	29.3

used in the DFMEX studies was *n*-heptane, which is a commercially available solvent. All chemicals were used as received. LIX79 and Cyanex 921 (TOPO) were kindly supplied free of charge by Henkel Corp. and Cytec Inc., Canada, respectively.

The hollow fiber module (HFM) is manufactured by Hoechst Celanese, Charlotte, NC (Liqui-Cel, 8 cm × 28 cm 5PCG-259 contactor and 5PCS-1002 Liqui-Cel Laboratory LLE) and details of contactors and hollow fiber membrane specifications are given in Table 1a and b.

2.2. Partition coefficients of Au(I)

The procedure adopted to determine the partition coefficient of Au(I) is described elsewhere [12].

2.3. Extraction equilibrium

The extraction of Au(I) by organic extractant LIX79 + TOPO dissolved in *n*-heptane has been studied and described elsewhere [12,13]. The value of extraction constant K_{ex} for Au(I) with LIX79 + TOPO was found to be $(3.14 \pm 0.15) \times 10^{13}$ [12,14].

2.4. Density and viscosity measurements

The density and viscosity of LIX79 + TOPO/*n*-heptane solutions were measured in order to relate the Au(I) extraction with their physical properties in the DFMEX process. The viscosity was measured at 25 ± 1 °C using a Cannon-Ubelhode semimicro 100 viscometer (Cannon Instruments Co., USA) and densities were determined by weighing a known volume of solution using a pycnometer.

2.5. DFMEX (with one module) setup

A schematic view of the membrane-based Au(I) extraction process (DFMEX) with LIX79 + TOPO/*n*-heptane using a hollow fiber contactor in recirculation mode is shown in Fig. 1. The aqueous and organic phases were contacted co-currently or counter-currently in a hollow fiber module for extraction or stripping runs in recirculating mode. In the extraction module, the feed aqueous phase flows (4.16–15.27 cm^3/s) through the lumen of the fibers, while the organic phase circulates (4.16–8.33 cm^3/s) through the shell side, wetting the wall of the hydrophobic fibers. The pressure in the aqueous phase was held 0.2–0.5 bar higher than the pressure in the organic phase [15,16]. In the stripping run, loaded organic extractant (LIX79 + TOPO with

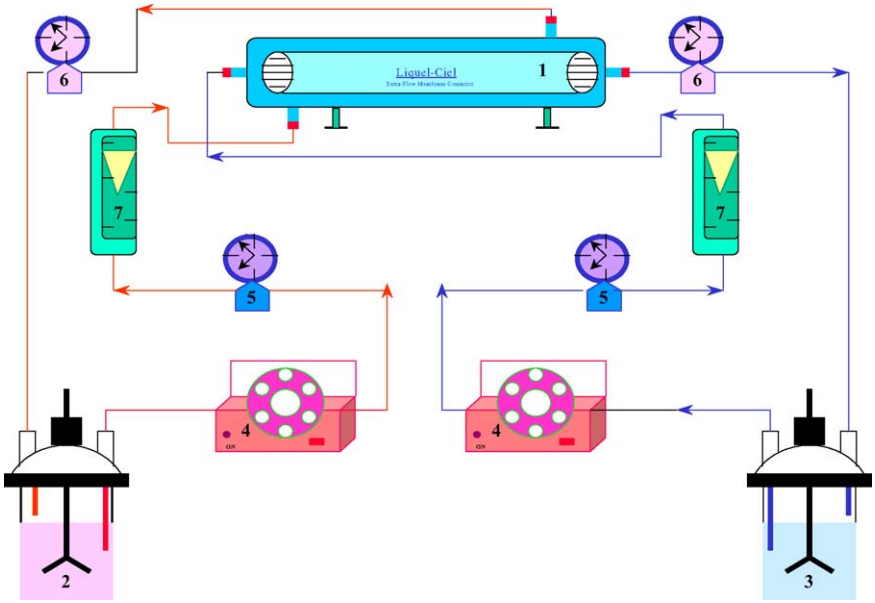

Fig. 1. A schematic view of the membrane-based extraction process of Au(I) from cyanide media using hollow fiber contactor. (1) Hollow fiber contactor; (2, 3) organic extractant and feed; (4) feed and organic pump; (5, 6) inlet and outlet pressure gauge, respectively, for organic and feed; (7) flowmeters for feed and organic.

gold complex) flowed through the shell side (4.72 cm^3/s), whereas 0.1–0.4 M NaOH flowed through the tube side (6.94 cm^3/s) counter-currently in recirculation mode.

The organic phase is a 1000 ml solution of 0.125 mol/dm^3 LIX79 + 0.125 mol/dm^3 TOPO in *n*-heptane. A quantity of 1000 ml of aqueous feed solution with the desired concentration of Au(I) was prepared by taking a suitable aliquot from the stock solution. Furthermore, the desired feed pH was reached by adding 1 mol/dm^3 NaOH solution. The Au(I) concentration in the feed was maintained at 2.5×10^{-4} mol/dm^3. The solution of 0.1–0.4 mol/dm^3 NaOH was used as the stripping phase when back extraction of Au(I) was carried out in the hollow fiber module. Small aliquots of the stripping stream and organic solution were taken at selected times for the analysis of metal concentration by standard atomic absorption spectrometry (2380 Perkin-Elmer Absorption Spectrometer).

2.6. IMP (with two module) setup

The integrated membrane process comprises two membrane modules, one for extraction and the other one for the back extraction (stripping) as well as a stirred tank for the organic solution and two stirred tanks for the aqueous phases. The experimental setup for the metal separation experiments consists of two gear pumps capable of flows of 1 l/min for the organic and BEX phases, powered by a variable speed dc motor, and a peristaltic pump for the feed aqueous phase capable of flows of 1 l/min. The organic phase wetted the porous wall of the fiber because of its hydrophobic nature. The interface was immobilized at the pore by applying a higher pressure to the aqueous stream than to the organic stream. The differential pressure was always kept below the breakthrough pressure. In the aqueous phase the pressure was held 0.2–0.5 bar higher than that in organic phase. A schematic view of the membrane-based solvent extraction and stripping process of Au(I) using two hollow fiber contactors in recirculation mode is shown in Fig. 1. The IMP operation was carried out with LIX79 and LIX79 + TOPO/*n*-heptane by contacting alkaline cyanide feed containing gold through tube side and organic extractant through shell side which was recirculated between extraction and stripping hollow fiber modules though shell side in counter-current mode. In second HF contactor, stripping solution (1 M NaOH) flowed through tube side in counter-current mode.

The organic phase is a 1500 ml solution of 0.125 M LIX79 + 0.125 M TOPO in *n*-heptane. One thousand milliliters of aqueous feed solution of desired concentration of Au(I) was prepared by taking suitable aliquot from the stock solution. Further, desired feed pH was adjusted by adding 0.4 M NaOH solution. The stripping solution, 0.4 M NaOH, was used when back extraction of Au(I) was carried out in hollow fiber module. At known times during the procedure, small aliquots of the feed stream (aqueous solution for the extraction and organic solution for the stripping) were taken and analyzed for metal concentration by standard atomic absorption spectrometry. Au(I) was stripped with 1 M NaOH for analyzing gold in organic phase.

3. Theoretical background

3.1. Non-dispersive membrane extraction

The mechanism for extracting gold with LIX79 + TOPO in the hollow fiber contactor is illustrated in Fig. 2. The following assumptions were made when developing the model: (i) the system is at steady state, (ii) pore size and wetting characteristics are uniform throughout the membrane, (iii) the curvature of the fluid–fluid interface does not significantly affect the rate of mass transfer, the equilibrium solute distribution or the interfacial area, (iv) no bulk flow correction is necessary, i.e. mass transfer is described adequately by simple film-type mass transfer coefficients, (v) no solute transport occurs through the non-porous parts of the membrane, (vi) the two fluids are virtually insoluble in each other and (vii) the equilibrium solute distribution is constant over the concentration range of interest.

As derived by Dahron and coworkers [17a,b], the key equation for the calculation of K^{E}_{Au} or K^{S}_{Au} for counter-current flow is:

$$\ln\left[\frac{C^0_{e/s}/H - C^0_f}{(C^0_{e/s}/H - C^0_f) + (V_f/HV_{e/s})(C^0_f - C_f)}\right] = t\frac{\begin{array}{c}[1 - \exp((-4K^E_{Au}V_m/d)(1/Q_f - 1/Q_{e/s}H))] \\ \times [1/V_f + 1/V_{e/s}H]\end{array}}{\begin{array}{c}(1/Q_f) - (1/Q_{e/s})\exp[(-4K^E_{Au}V_m/d) \\ \times (1/Q_f - 1/Q_{e/s}H)]\end{array}} \quad (1)$$

where Q_f and $Q_{e/s}$ are the feed and extract/strip flow rates, V_f and $V_{e/s}$ the feed and extract/strip volumes, C^0_f and $C^0_{e/s}$ the concentrations of the solute in the feed and in the extract/strip solutions at a given instant ($t = 0$), C_f the concentration of the solute at the instant t, V_m the volume of all the hollow fibers and d the internal diameter of one fiber.

4. Model development

In DFMEX and IMP, the system consists of an aqueous phase containing $Au(CN)_2^-$ flowing through the tube side of microporous hollow fiber membranes whose pores are filled with the organic extractant (LIX79 + TOPO/*n*-heptane), and the organic extractant was flowing counter-currently through the shell side (Fig. 1). The extraction reaction takes place at the inside wall of the membrane where the phase interface is located (Fig. 2). To determine the rate-controlling step, we consider the commonly used hypothesis that the extraction involves four sequential steps: effective rate of interfacial reaction at the interface between two phases, mass transfer

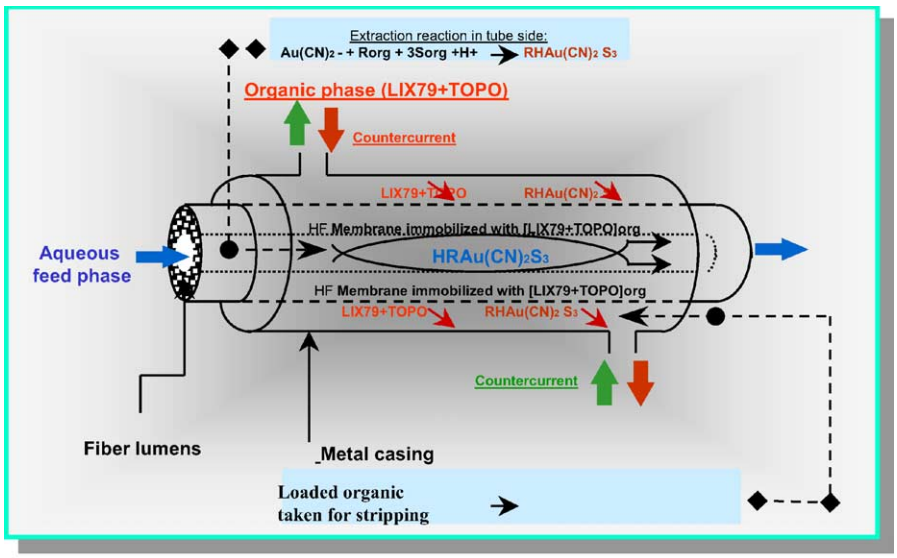

(a)

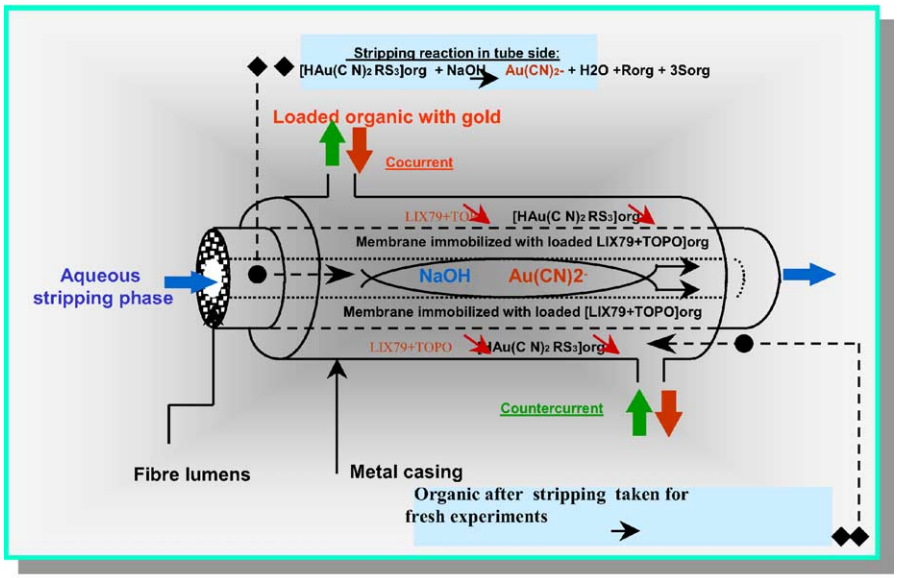

(b)

Fig. 2. (a) Extraction mechanism of gold cyanide with LIX79 + TOPO in single hollow fiber contactor and (b) stripping mechanism of gold cyanide with LIX79 + TOPO in single hollow fiber contactor.

from the bulk aqueous feed to the inside surface of the hollow fiber membrane, diffusion across the porous membrane itself and mass transfer into the organic solution surrounding the fiber. In the stripping module, gold complex from bulk of organic (LIX79 + TOPO) phase is transferred first to the membrane–strip interface at the pore mouth and finally to the bulk aqueous stripping phase [18].

Assuming a resistance in the series model [16], the reciprocal of the overall mass transfer coefficient is the total resistance to mass transfer and can be described as the sum of the mass transfer resistances inside the fibers (feed phase), across the fiber wall (membrane resistance) and outside the fibers (organic phase), and resistance caused by interfacial reaction. Therefore, the expression for the overall mass transfer coefficient, K^{E}_{Au}, can be written as [19,20]

$$\frac{1}{K^{E}_{Au}} = \frac{1}{k_i} + \frac{1}{k_f} + \left(\frac{d_i}{d_{lm}}\right)\frac{1}{k_m H} + \left(\frac{d_i}{D_h}\right)\frac{1}{k_s H} \quad (2)$$

The following expression takes into account the empirical relations for k_f and k_s, which depend on the hydrodynamics of the feed and organic phases, respectively:

$$\frac{1}{K^{E}_{Au}} = \frac{1}{k_i} + \frac{1}{(D_t/d_i)(d_i^2 \upsilon_t / L D_t)^{1/3}} + \left(\frac{d_i}{d_{lm}}\right)\frac{\tau t_m}{K_{ex}[H^+][R_{org}][S_{org}]^3 (D_m \varepsilon)}$$

$$+\left(\frac{d_i}{D_h}\right)\frac{1}{K_{ex}[H^+][R_{org}][S_{org}]^3\beta L \times (\upsilon_s D_h/\eta_s)^{0.6}(\eta_s/D_s)^{0.33}(D_s/D_h)} \quad (3)$$

where

$$\frac{1}{k_i} = \frac{1}{k_e[H^+][R_{org}][S_{org}]^3} \quad (4)$$

and $H = K_{ex}[H^+][R_{org}][S_{org}]^3$, thus $[H^+][R_{org}][S_{org}]^3 = H/K_{ex}$.

After suitable substitution in Eq. (4),

$$\frac{1}{k_i} = \frac{1}{k_e[H/K_{ex}]}$$

and k_i is the effective rate of interfacial reaction at the surface, k_f, k_m and k_s the mass transfer coefficients in the aqueous feed, membrane and organic solvent, respectively, and d_i, D_h and d_{lm} the internal, external and logarithmic mean fiber diameters, respectively. Eq. (4) was derived to estimate the value of k_i using a method similar to those found in the literature [18,21,22]. The partition coefficient, $H = K_{ex}[H^+][R_{org}][S_{org}]^3$, appears in the membrane resistance, because in our experiments the organic solvent wets the membrane but water does not.

The overall mass transfer coefficient can be calculated from the individual transfer coefficients k_i, k_f, k_m and k_s. The tube and shell side mass transfer coefficients are known to depend on the flow conditions in the fiber lumen and shell fluid, respectively, and correlations are available in the literature expressing these dependencies.

The flow through the fibers in the membrane modules will always be laminar. For this reason, the individual mass transfer coefficient for the tube side is dependent on the mean flow velocity υ_f, according to Refs. [23–25]:

$$N_{Sh} = \frac{k_f d_i}{D_t} = 1.64\left(\frac{D_t}{d_i}\right)\left(\frac{d_i^2\upsilon_f}{LD_t}\right)^{1/3} \quad (5)$$

This is the well-known Lévêque solution (only the constant is changed to 1.62 in Eq. (5)) applicable when the Graetz number is large [20,26a–e]. Also, Eq. (5) overestimates experimentally determined mass transfer coefficients at low flows; this can be attributed to non-uniform flow caused by polydispersity in hollow fiber diameter [26f]. To be precise, the above correlation predicts mass transfer coefficients with reasonable accuracy for $N_{Gz} > 4$ but overestimates them for $N_{Gz} < 4$ [26a]. In the experimental conditions described here, N_{Gz} ranges between 5.5 and 8.2. Also one need to be very careful while applying Lévêque equation, as flow of fluid in tube is considered to be laminar. Park and Chang [26g] showed that tube side flow distribution is non-uniform. Using high-speed photography and dye tracer studies, these researchers determined that the distribution depends on the inlet manifold type (cylindrical or conical), manifold height, tube length, fiber inner diameter, shell diameter, fiber packing density and Reynolds number. Nearly uniform flow was achieved for certain shell and tube geometries with long manifolds at low Reynolds numbers; however, non-uniform flow was the rule rather than the exception.

Similarly, for the shell side mass transfer coefficient, the following correlation has been given [17,23,27]:

$$N_{Sh} = \frac{k_s D_h}{D_s} = \beta\left[\frac{D_h(1-\phi)}{L}\right]N_{Re}^{0.6}N_{Sc}^{0.33} \quad (6)$$

where $N_{Re} = \upsilon_s D_h/\eta_s$, $N_{Sc} = \eta_s/D_s$, $\beta = 5.85$ for hydrophobic membranes, $0 < N_{Re} < 500$ and $0.04 < \phi < 0.4$. In this system both conditions are fulfilled, as N_{Re} ranges between 3.0 and 11.0 and $\phi = 0.35$. D_h is the hydraulic diameter, D_t the diffusion coefficient of the solute on the tube side, d_i the inner fiber diameter, d_o the outer fiber diameter, L the fiber length, D_s the diffusion coefficient of the solute on the shell side, and υ_t and υ_s the velocities of the liquid on the fiber side and shell side, respectively. An estimate of the membrane mass transfer coefficient can be determined by the following equation [28,29]:

$$k_m = \frac{D_m\varepsilon}{\tau(d_o - d_i/2)} \quad (7)$$

For the membrane and solvent considered here, membrane thickness (t_m) = 30 μm; tortuosity (τ) = 3 (value obtained from Celgard GmbH); diffusion coefficient of the gold complex in the membrane (D_m) = 2.6×10^{-6} cm^2/s [12]; ε = 0.30; and H = 36.9. The membrane tortuosity was also determined by the Wakao–Smith relation, expressed as the inverse of the membrane porosity, which almost matches the value suggested by Hoechst Celanese (now known as Celgard GmbH) [30].

The membrane mass transfer coefficient does not depend on the hydrodynamics; it is only related to the membrane properties and to the diffusion coefficient of the solute in the organic phase present in the pores.

5. Results and discussion

5.1. Gold cyanide–LIX79 + TOPO extraction system

The LIX79 + TOPO (4% (v/v) or 0.125 M each) system was observed to enhance the kinetics of the system as indicated in Figs. 3 and 4. The lower concentration of LIX79 (0.125 M) with TOPO (0.125 M) afforded a very promising performance as compared to 0.375 M of LIX79 alone (Fig. 3). It took 300 s to extract more than 95% gold with LIX79 + TOPO (0.125 M), whereas pure LIX79 (0.375 M) (12% (v/v)) took 1860 s to reach the same percentage value of gold extraction (Fig. 4). For this reason, more systematic studies were planned in order to optimize the hydrodynamic and chemical conditions and thus obtain an improved methodology with LIX79 + TOPO. The diluent for this DFSX system was selected on the basis of previous studies

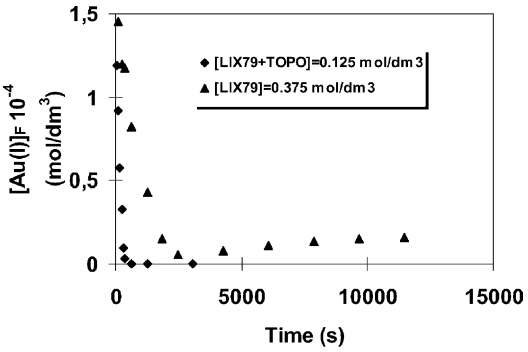

Fig. 3. Extraction (%) of gold cyanide using LIX79 + TOPO and LIX79 alone.

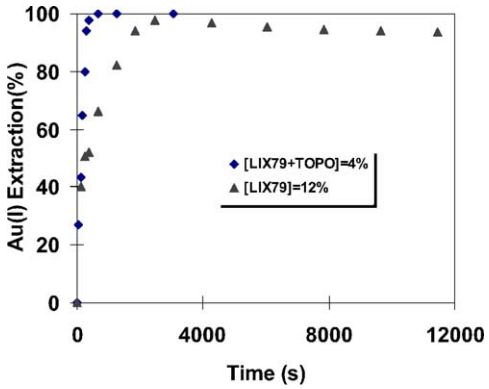

Fig. 4. Variations of gold cyanide concentration in feed as a function of time for LIX79 + TOPO and LIX79 alone.

performed with *n*-heptane [3,4,11]. The physical properties and equilibrium parameters required to calculate the mass transfer coefficient are presented in Table 2. In the DFSX technique, it is well established [2,3] that, in order to keep the interface within the pores of a hydrophobic membrane, it is necessary to maintain a higher local pressure in the aqueous phase. Fig. 5 shows a typical plot of concentration differences versus time as predicted by Eq. (1) for extraction of Au(I) into LIX79 + TOPO. In this plot, the Au(I) concentration varies semi-logarithmically with time. From these plots, the overall mass transfer coefficient, K^{E}_{Au}, can be calculated. The results of these calculations are given in Tables 3 and 6. The mass transfer coefficients K^{E}_{Au} for the extraction varied from 1.7×10^{-6} to 6.9×10^{-6} cm/s. Table 3

Table 2
Physical conditions and equilibrium parameters

Symbol	Property	Value
H	Partition coefficient	36.9, 0.16[a]
D_m	Pore liquid diffusivity (cm^2/s)	2.6×10^{-6}
D_s	Shell liquid diffusivity (cm^2/s)	2.6×10^{-5}
D_t	Aqueous diffusion coefficient of Au(I) (cm^2/s)	7.6×10^{-6}
η_s	Shell fluid viscosity (g/cm s)	4.31×10^{-3}, 3.87×10^{-3} [b]
K_{ex}	Extraction equilibrium constant	$(3.14 \pm 0.15)\times10^{13}$
k_e	Forward reaction rate constant of Eq. (4) (cm/s)	9.7×10^{10}
k_i	Effective rate of interfacial reaction (cm/s)	7.9×10^{-7}

[a] Partition coefficient for stripping.
[b] Viscosity of diluent *n*-heptane.

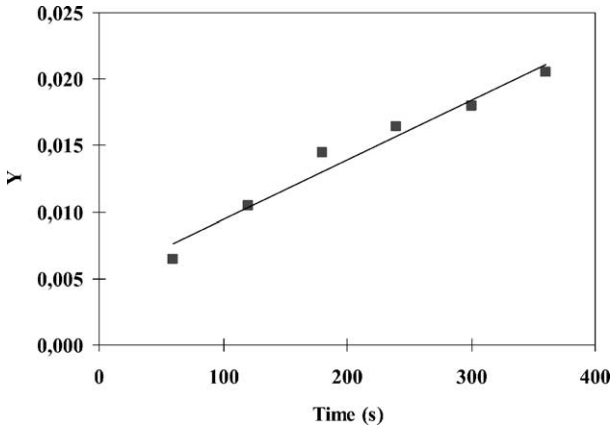

Fig. 5. Concentration courses of Au(I) (Y = LHS of Eq. (1)) extraction obtained from Eq. (1) vs. time (t).

shows K^{E}_{Au} values from alkaline cyanide media using LIX79 (0.375 M) alone and equimolar 0.125 M LIX79 + 0.125 M TOPO in *n*-heptane under similar experimental conditions at pH 10.3. The K^{E}_{Au} value was around four times higher with an equimolar mixture of 0.125 M LIX79 + 0.125 M TOPO than with LIX79/*n*-heptane alone. This is probably due to the increased basicity of LIX79 as a result of the addition of TOPO. Similar mechanism has been suggested by Mooiman and Miller [9] while carrying out extraction of Au(I) by modified amines with organophosphorous extractants. TOPO alone can also extract gold cyanide from alkaline cyanide media by a solvation reaction mechanism

Table 3
DFSX technique with single module in counter-current mode: mass transfer coefficients for extraction of Au(I) from aqueous alkaline cyanide media with equimolar LIX79 + TOPO (0.125 M) and LIX79 (0.375 M) alone in *n*-heptane

Extractants	[LIX79] = 0.375 M (mol/dm^3)		[LIX79 + TOPO] = 0.125 M (mol/dm^3)	
Q_f (cm^3/s)	6.94	15.27	6.94	15.27
Q_e (cm^3/s)	4.72	4.72	4.72	4.72
K^{E}_{Au}	1.0×10^{-6}	5.8×10^{-6}	4.3×10^{-6}	6.9×10^{-6}
Extraction (%)	100	98	87	100

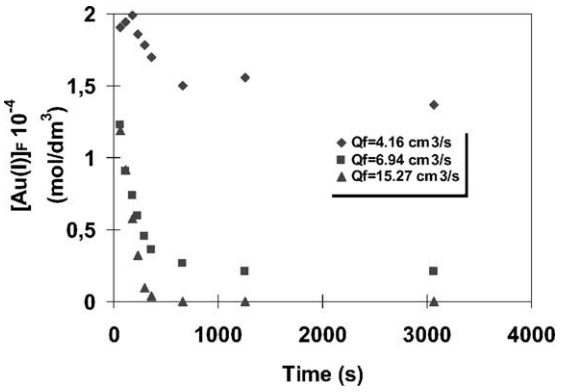

Fig. 6. Variations of gold cyanide concentration in feed as a function of time for different aqueous flow rate in counter-current mode using LIX79 + TOPO/*n*-heptane.

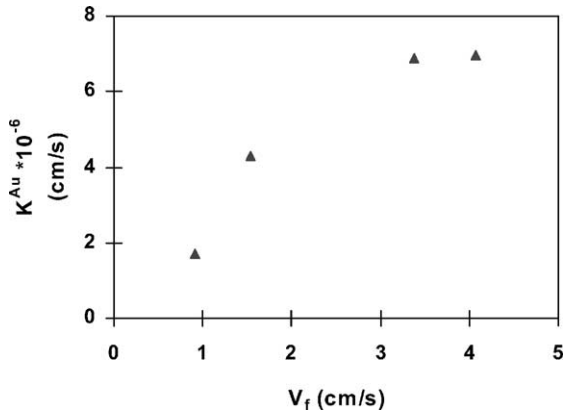

Fig. 7. Effect of feed flow rate on mass transfer coefficient of gold cyanide with LIX79 + TOPO in extraction module in counter-current mode.

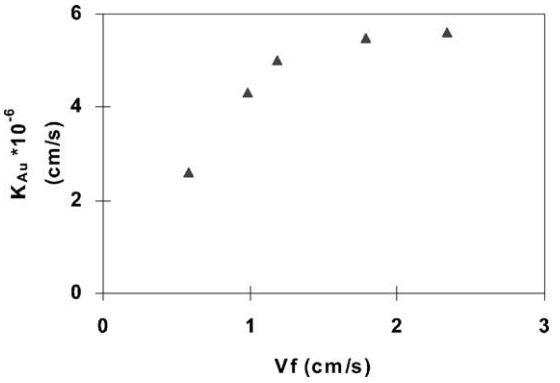

Fig. 8. Variations of gold cyanide concentration in feed as a function of time for different organic flow rate in counter-current mode using LIX79 + TOPO/*n*-heptane.

$(M^+ \cdots Au(CN)_2 \cdot S_n)$, as suggested by Mooiman and Miller [9]. The K^E_{Au} value was found to be 2.1×10^{-6} cm/s with TOPO alone, whereas the value with LIX79 was 1.0×10^{-6} cm/s. Interestingly, LIX79 + TOPO yielded a value of K^E_{Au} of 6.9×10^{-3} cm/s, which is around three times higher than when TOPO was used alone and around seven times more gold than when pure LIX79 was employed without the addition of TOPO.

Variations of gold cyanide concentration in the feed as a function of time for different aqueous feed flow rates in counter-current mode are shown in Fig. 6. The performance of the extraction module was not good when the Reynolds number was 2.2 or below. When the Reynolds number was increased to 3.67, the performance started to improve, and was observed to be best at Reynolds number 8.09. Table 4 and Fig. 7 present the influence of linear flow velocity on K^E_{Au}; its values increased with linear flow velocity ranging between 0.92 and 3.37 cm/s, and no further increase in flow rates was checked. For example, when linear flow velocity (υ_f) was varied by a factor of 3, the overall mass transfer coefficient (K^E_{Au}) increased by four times. The values of k_f calculated theoretically from Eq. (5) were around two orders of magnitude higher than K^E_{Au}. Hence, the feed resistance ($1/k_f$) does not dominate the overall mass transfer coefficient. In earlier studies with Au(I) [3], Au(I) removal from the feed phase was found to be faster in counter-current mode. Therefore, all the studies were carried out in counter-current mode.

Fig. 8 depicts variations of gold cyanide concentration in the feed as a function of time for different organic flow rates in counter-current mode. These data in the figure show the effect of changing the shell side organic phase flow rate and keeping the aqueous flow rate constant for equimolar LIX79 + TOPO (0.125 M) in *n*-heptane. Module extraction efficiency changed dramatically below Reynolds number = 9.0 and improved significantly when Reynolds number increased from 18.3 to 22.7 (Table 5). This means that most of the gold cyanide can be easily transferred into the organic phase through the interfacial reaction when the concentration of the LIX79 is in excess due to an increase in the organic phase flow rate, since the aqueous inlet concentration of gold is only 2.5×10^{-4} mol/cm^3 and the aqueous stream flow rate, Q_f, is around 11.1 cm^3/s (υ_f = 2.5 cm/s).

Table 4
DFSX technique with single module in counter-current mode: mass transfer coefficients for extraction of Au(I) from aqueous alkaline cyanide media with equimolar LIX79 + TOPO (0.125 M) in *n*-heptane as a function of aqueous flow rates

Experiment number	Q_e (cm^3/s)	Q_f (cm^3/s)	υ_f (cm/s)	Reynolds number	K^E_{Au} ($\times 10^{-6}$ cm/s)	k_f calculated from Eq. (5) (cm/s)	$1/k_f$ (S/cm)
1	4.72	4.16	0.92	2.20	1.7	2.9×10^{-4}	3.4×10^3
2	4.72	6.94	1.53	3.67	4.3	3.4×10^{-4}	2.9×10^3
3	4.72	15.27	3.37	8.09	6.9	6.0×10^{-4}	1.7×10^3

Table 5
DFSX technique with single module in counter-current mode: mass transfer coefficients for extraction of Au(I) from aqueous alkaline cyanide media with equimolar LIX79 + TOPO (0.125 M) in *n*-heptane as a function of organic flow rates

Experiment number	Q_f (cm^3/s)	Q_e (cm^3/s)	υ_f (cm/s)	Reynolds number	K^E_{Au} ($\times 10^{-6}$ cm/s)	k_s calculated from Eq. (6) (cm/s)	$1/k_s$ (S/cm)
1	11.11	4.16	0.39	9.04	2.6	10.9×10^{-5}	9.1×10^3
2	11.11	6.94	0.79	18.33	4.3	15.6×10^{-5}	6.4×10^3
3	11.11	8.33	0.98	22.73	5.0	17.4×10^{-5}	5.7×10^3

Thus, the shell side resistance is negligible beyond an organic flow rate of 11.1 cm^3/s. Fig. 9 depicts the effect of the organic flow rate on the mass transfer coefficient as a function of linear flow velocity in counter-current mode using LIX79 + TOPO/*n*-heptane. As indicated by Eq. (6), the organic mass transfer coefficient was expected to increase with linear flow velocity ($N_{Re} = \upsilon d/\eta$). The increasing trend with linear flow velocity was observed up to around 1.00 cm/s and further high flow rates were not checked, as results were quite promising with the applied flow rates of organic solutions. The increase in the mass transfer coefficient with flow rate was found particularly up to a point (1.00 cm/s) and then flattened off indicating that resistance in that particular phase was no longer controlling and that the control had switched to a reaction mechanism.

The effect of pH variation was not investigated in this study, as earlier work with LIX79+TOPO indicated that gold extraction remained almost constant with increases in pH up to 11 but decreased with a further increase in pH, i.e. 12 [12]. This is probably due to the role played by hydrogen ions in gold complex formation with the mixture of LIX79 and TOPO, which is not favorable when the pH of the aqueous solution reaches 12. The aqueous feed was deliberately set at pH 10.3, considering that real hydrometallurgical solutions have a pH between 10.0 and 10.5. Similarly, the effect of NaCN with the LIX79+TOPO system revealed that gold extraction remained constant when the concentration of NaCN varied between 200 and 500 ppm. The cyanide concentration studied in the working range did not cause any competition with $Au(CN)_2^-$ [12]. Nevertheless, while performing gold

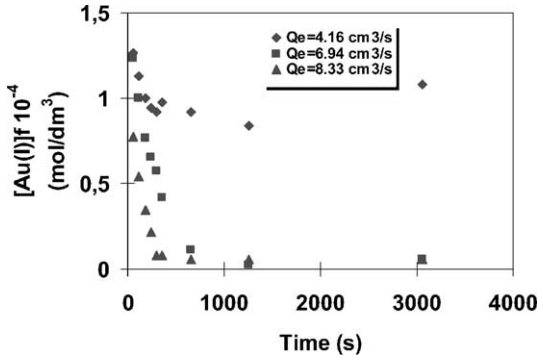

Fig. 9. Effect of organic flow rate on mass transfer coefficient as a function of linear flow velocity in counter-current mode using LIX79 + TOPO/*n*-heptane.

recovery from a typical mine solution with LIX79, Viring et al. reported that a very high concentration of NaCN can compete with the gold and can result in a reduction in gold recovery. The studies performed by our group with LIX79 alone (0.375 M) revealed that the concentration of LIX79 can be increased in order to mitigate the effect of increased NaCN concentration competing with gold cyanide [13].

The first term in Eq. (2) presents the local value of the total resistance. This resistance is in turn the sum of the mass transfer resistances inside the fiber, across the fiber wall and in the solution surrounding the fiber. The value of $[R]_{org}[H^+]_{aq} = \theta$ is 10^{-16} to 10^{-18}. The value of k_i was around 7.9×10^{-7} cm/s and k_s was between 10.9×10^{-5} and 17.4×10^{-5} cm/s, whereas k_m was about 8.66×10^{-5} cm/s. The value of k_f ranged between 2.9 and 6.0×10^{-4} cm/s. Therefore, on the right hand side of Eq. (2), the first term is around 1.3×10^6, the second term is around (2–3) $\times 10^3$, the third term is around 250 and the fourth term ranges from 37 to 60 S/cm. The overall resistance in the experiments calculated from Eq. (1) was observed to be (2–6) $\times 10^6$ S/cm, as compared to an overall resistance value of 1.2×10^6 S/cm estimated from the model, which shows that the resistance due to reaction at the interface is dominant at high flow rates of extractant and feed. The second, third and fourth terms are thus negligible. In this respect, the fractional resistance of each step of the overall process, R^0_m, R^0_f, R^0_s and R^0_i, can be calculated; for example, R^0_m can be calculated by the following equation:

$$R^0_m = R_m/(R_i + R_m + R_s + R_f) \quad (8)$$

where R_i, R_m, R_s and R_f are mass transfer resistances due to interfacial reaction, membrane, organic extractor and feed. Under the experimental conditions studied, the values of R^0_m, R^0_f, R^0_s and R^0_i were 0.02, 0.27, 0.01 and 99.70%, respectively. This clearly indicated that the rate-controlling step was the interfacial reaction on the membrane surface.

The differences in the theoretical and the experimentally observed N_{Sh} (mass transfer coefficient) and N_{Re} may be attributed to several causes. This could be due to several reasons as explained by several researchers [2–4,20,23,26g,31–36]. In hollow fiber contactor, the tube side flow regime is likely to be laminar due to very small lumen diameter. Otherwise, the pressure drop along the fiber would be exceedingly high. In any such correlation developed, the effects of any maldistribution of flow on the tube side resulting from particular design of inlet and outlet

headers are hidden [26g,32]. Similarly, the effects of any fiber inlet crimping or fiber inlet plugging at the tube sheet are unknown. On the other hand, hollow fiber modules usually exhibit channeling, bypassing and stagnant regions on the shell side due to non-uniform distribution of the fibers and its elongation by the use of organic solvents [33–35]. The hydrodynamics of the organic phase circulating in the shell side will be affected by these deviations from ideal flow, thus causing an incorrect evaluation of mass transfer coefficient. This deviation could also be due to the inaccuracy associated with evaluation of diffusion coefficient of solute in organic phase which is directly linked to Eqs. (5)–(7). Therefore, inaccuracy in diffusion coefficient values can result in significant deviation of mass transfer coefficients [31].

5.2. Gold cyanide–LIX79 stripping system

Stripping was performed separately in a single module by circulating loaded organic solution (LIX79 + TOPO with metal complex) on the shell side and NaOH solution on the tube side. Linear plots were obtained from Eq. (1) for the stripping of Au(I) from LIX79 + TOPO into aqueous NaOH. Fig. 10 shows a typical plot of concentration differences versus time as predicted by Eq. (1) for the stripping of Au(I) from LIX79 + TOPO–goldcyanide complex by 0.4 M NaOH. The mass transfer coefficients for the stripping (K^{S}_{Au}) were calculated by multiplying with the reversed partition coefficient (H), as the mass transfer driving force is in the opposite direction to forward extraction. The overall mass transfer coefficients (K^{S}_{Au}) for stripping ranged from 0.43×10^{-5} to 1.7×10^{-5} cm/s. Table 6 shows that there was a clear reduction in gold recovery when the concentration of NaOH was less than 0.4 M. This may be due to an incomplete stripping reaction in the 0.1 M NaOH. Therefore, NaOH concentration was raised to 0.4 M and stripping (%) was around 100. The values of K^{S}_{Au} were found to be of the same order of magnitude regardless of the contacting mode (co-current or counter-current) for the stripping

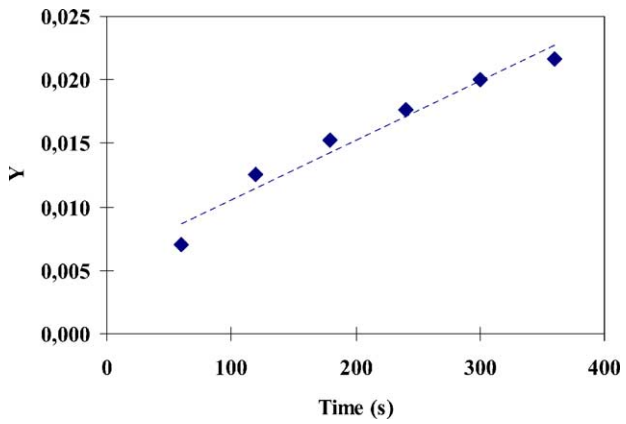

Fig. 10. Concentration courses of Au(I) stripping obtained from Eq. (1) vs. time (t) (Y = LHS of Eq. (1)).

Table 6
DFSX technique with single module in counter-current mode: mass transfer coefficients for extraction of Au(I) from aqueous alkaline cyanide media with equimolar LIX79 + TOPO (0.125 M) in *n*-heptane as different NaOH concentrations

Experiment number	[NaOH] (mol/dm^3)	K^{E}_{Au} ($\times 10^{-5}$ cm/s)	r^2	Stripping (%)
1	0.1	0.43	0.99	80
2	0.2	1.70	0.95	100

experiments. The rate of stripping reaction at the surface was not considered in the stripping experiments. The reaction is instantaneous and fast, which was also confirmed when the overall mass transfer coefficient was estimated to be of the same order as that predicted by the model using k_f, k_m and k_s without placing k_i term in Eq. (9). Also, stripping is taking place due to the shift of equilibrium which takes place when pH of the solution is maintained between 13 and 14. In this pH range, there is no possible extraction reaction in stripping side. The most favorable extraction is taking place in pH range 9–10 due to protonation of LIX79 (RH^+).

The following equation could be used to calculate the overall mass transfer coefficients for the stripping [31]:

$$\frac{1}{K^{S}_{Au}} = \frac{1}{k_s} + \frac{1}{k_m} + \frac{1}{k_{st}H} \tag{9}$$

where k_s, k_m, k_{st}, H, $1/K^{S}_{Au}$, $1/k_s$, $1/k_m$ and $1/k_{st}H$ are defined in the list of notations. For gold extraction, the partition coefficient appears in the first and second terms, but it does not for gold stripping. This occurs because of the wetting situation for the membrane. The membrane is wetted by the organic solvent in the case of gold extraction. Moreover, the solvent has a higher solubility for the solute. For gold stripping, the membrane is also wetted by the organic solvent, but in this case it is the solvent which has the lower solubility for the solute [31].

Eq. (9) indicates that the overall resistance for stripping is the sum of local values of the individual resistances. The value of k_s (precision given with a maximum of 10% error) for the organic feed was around 10.9×10^{-5} cm/s (calculated from Eq. (6)), whereas k_m was around 8.66×10^{-5} cm/s (calculated from Eq. (7)), as determined earlier for extraction studies. The value of k_{st} was around 3.4×10^{-4} cm/s (calculated from Eq. (5)). Therefore, on the right hand side of Eq. (2), the first term is around 9.2×10^3 S/cm, the second term is around 11.5×10^3 S/cm and the third term is around 3.7×10^3 S/cm. The overall resistance in the experiments calculated from Eq. (1) was observed to be 5.8×10^4 S/cm, as compared to the value of overall resistance, 2.4×10^4 S/cm, estimated from the model (Eq. (9)), which shows that the resistance due to membrane and organic mass transfer is dominant under the experimental conditions studied. In this respect, the fractional resistances of each step in the overall process, R^0_m, R^0_s and R^0_{st}, can be calculated; for example,

R_m^0 can be calculated by the following equation:

$$R_m^0 = R_m/(R_s + R_m + R_{st}) \quad (10)$$

where R_m, R_s and R_{st} are the mass transfer resistances due to membrane, organic extractant and aqueous strip. Under these experimental conditions, the values of R_m^0, R_s^0 and R_{st}^0 were 37.7, 47.3 and 15%, respectively. This clearly indicates that the rate-controlling steps were in the membrane and organic solution. The membrane resistance can be minimized if stripping is carried out in hollow fiber contactors containing hydrophilic membranes.

No significant deviation of the mass transfer coefficients was observed during extraction, as interfacial reaction was dominant throughout the entire extraction process, and mass transfer correlations were not of much use because the influence of the flow rate on mass transfer was negligible. On the other hand, in the stripping experiments, this deviation was more pronounced, as stripping is more influenced by the organic flow rate on the shell side. This behavior could be attributable to an irregular flow on the shell side caused by the existence of stagnant zones, preferential pathways and deficient mixing due to a non-uniform distribution of fibers and to their possible deformation by the action of the organic solvent [33–35]. These effects are important mainly when commercial modules are used, since the fibers are not uniformly spaced. Also, the poor distribution of the shell side flow due to the random packing of fibers in the module bundle probably contributed to the inaccuracy of shell side mass transfer coefficients, as observed by Rogers and Long [36].

6. Conclusions

The mixture of LIX79 + TOPO affords a better performance than LIX79 alone. Therefore, to obtain a high mass transfer coefficient, the dispersion-free solvent extraction mode was selected. The DFSX system with mixed reagent improved the kinetics of the whole system by employing LIX79+TOPO as extractant and a stable performance was obtained. The results obtained with the LIX79 + TOPO and LIX79 alone are compared in order to justify the improvement in the system. The overall mass transfer coefficients for extraction (K_{Au}^E) and stripping (K_{Au}^S) of Au(I) were calculated to be 6.9×10^{-6} cm/s and 1.7×10^{-5} cm/s, respectively. The equimolar concentration of LIX79 + TOPO yielded the value of K_{Au}^E as 6.9×10^{-3} cm/s, which is around three times more than when TOPO was used alone and around seven times more gold than when pure LIX79 was employed without the addition of TOPO. The following advantages were noted with the DFSX system described here: (a) less consumption of LIX79 extractant, (b) faster extraction and stripping, (c) no interference from NaCN [12] and (d) no pH dependency [12].

The separation and recovery of gold in the presence of other metal cyanide salts of Fe(II), Cu(I), Ni(II), Ag(I) and Zn(II) from alkaline cyanide solutions using LIX79 + TOPO/*n*-heptane is not carried out in this study, as this is already described in our earlier publication. The selectivity of Au(I) with respect to Zn(II) and Ag(I) cyanide salts was also found to be improved [12]. A model is presented which describes the extraction mechanism, indicating different rate-controlling steps. The mass transfer resistance, which resulted from a chemical extraction reaction at the surface, was observed to be dominant throughout the entire extraction process, whereas the stripping reaction was fast and instantaneous and the model clearly indicated that the rate-controlling step in the stripping module was in the membrane and the organic solution. The resistance of the membrane can also be minimized if hydrophilic membranes are used instead of hydrophobic membranes in the stripping module. The validity of this model was evaluated with experimental data and found to tie in well with theoretical values.

Acknowledgements

This work was supported by the CICYT (PPQ2002-04267) and DURSI (SGR2001-249). Dr. Anil Kumar Pabby acknowledges the financial support of the Comisión Interministerial de Ciencia y Tecnología, Spain, through the award of a Visiting Scientist Fellowship. R. Haddad acknowledges the fellowship granted by the ICMA. G. Benzal acknowledges a fellowship awarded by the FOMEC (Fondo para la Mejora de la Enseñanza y Calidad Universitaria) of the Universidad Nacional de Tucumán, Tucumán, Argentina. The authors would also like to thank the Henkel Corporation, USA, for supplying the LIX79.

References

[1] J.L. Cortina, E. Meinhardt, O. Roijals, V. Marti, Modification and preparation of polymeric adsorbents for precious-metal extraction in hydrometallurgical processes, React. Polym. 36 (1998) 149.
[2] A. Kumar, A.M. Sastre, Non-dispersive membrane extraction–separation process developments, in: A.K. SenGupta, Y. Marcus (Eds.), Ion Exchange and Solvent Extraction, vol. 15, Marcel Dekker, New York, 2001, Chapter 8, pp. 313–469.
[3] A. Gableman, S.-T. Hwang, Hollow fiber membrane contactors, J. Membr. Sci. 159 (1999) 61.
[4] A. Kumar, R. Haddad, A.M. Sastre, Integrated membrane process for recovery of gold cyanide with LIX79 from hydrometallurgical solutions: modeling and performance evaluation, AIChE J. 47 (2001) 328.
[5] A. Kumar Pabby, R. Haddad, G. Benzal, A.M. Sastre, Dispersion-free solvent extraction and stripping of gold cyanide with LIX79 using hollow fiber contactors: optimization and modelling, Ind. Eng. Chem. Res. 41 (2002) 613.
[6] A. Kumar, A.M. Sastre, Novel membrane based processes for recovery of gold from cyanide media using hollow fiber contactors: impregnation and non-dispersive membrane extraction mode, Spanish Patent 9801736.
[7] A. Kumar, A.M. Sastre, Hollow fiber membrane process: a promising approach to environmental and hydrometallurgical applications, in:

Proceedings of the International Solvent Extraction Conference (ISEC'99), July 11–16, 1999, Barcelona, Spain.
[8] A. Kumar, A.M. Sastre, Hollow fiber supported liquid membrane for the separation/concentration of gold(I) from aqueous cyanide media modeling and mass transfer evaluation, Ind. Eng. Chem. Res. 39 (2000) 146.
[9] M.B. Mooiman, J.D. Miller, The chemistry of gold solvent extraction from cyanide solutions using modified amines, Hydrometallurgy 16 (1986) 245;
M.B. Mooiman, J.D. Miller, A review of new developments in amine solvent extraction systems for hydrometallurgy, Sep. Sci. Technol. 19 (1984) 895.
[10] M.B. Mooiman, J.D. Miller, The solvent extraction of gold from aurocyanide solutions, in: Proceedings of the International Solvent Extraction Conference (ISEC'83), AIChE, New York, NY, 1983, p. 530.
[11] M.B. Mooiman, J.D. Miller, Selectivity considerations in the amine extraction of gold from alkaline cyanide solutions, Miner. Metall. Process SHE/AIME (August 1984) 153.
[12] A. Kumar Pabby, R. Haddad, G. Benzal, R. Ninou, A.M. Sastre, Use of modified membrane carrier system for recovery of gold cyanide from alkaline cyanide media using hollow fiber supported liquid membranes: feasibility studies and mass transfer modelling, J. Membr. Sci. 174 (2000) 17.
[13] R. Haddad, Procesos de recuperación de metales mediante membranas en configuración de fibra hueca: aplicación a la separación/concentración de AuI y AgI de disoluciones cianuradas, Ph.D. Thesis, Universitat Politècnica de Catalunya, Barcelona, Spain, October 2002.
[14] A. Kumar, R. Haddad, R. Ninou, A.M. Sastre, Solvent extraction of gold cyanide with modified extractants (LIX79 + TOPO), Solvent Extr. Ion Exc., submitted for publication.
[15] A. Kiani, R.R. Bhave, K.K. Sirkar, Solvent extraction with immobilized interfaces in a microporous hydrophobic membrane, J. Membr. Sci. 20 (1984) 125.
[16] Ho W.S. Winston, K.K. Sirkar, Membrane Handbook, Van Nostrand Reinhold, New York, 1992.
[17] (a) N.A. D'Elia, L. Dahron, E.L. Cussler, J. Membr. Sci. 29 (1986) 309;
(b) L. Dahron, Designing liquid–liquid extraction in hollow fiber modules, Ph.D. Thesis, University of Minnesota, 1987.;
(c) L. Dahron, E.L. Cussler, AIChE J. 34 (1988) 130–136.
[18] C.H. Yun, R. Prasad, A.K. Guha, K.K. Sirkar, Hollow fiber solvent extraction removal of toxic heavy metals from aqueous waste streams, Ind. Eng. Chem. Res. 32 (1993) 1186.
[19] E.L. Cussler, Diffusion, Cambridge University Press, London, 1984.
[20] E.L. Cussler, Hollow fiber contactors, in: J.G. Crespo, K.W. Boddeker (Eds.), Membrane Processes in Separation and Purification, Kluwer Academic Publishers, Dordrecht, 1994.
[21] C. Yang, E.L. Cussler, Reaction dependent extraction of copper and nickel using hollow fibers, J. Membr. Sci. 166 (2000) 229.
[22] Z.-F. Yang, A.K. Guha, K.K. Sirkar, Novel membrane based synergistic metal extraction and recovery process, Ind. Eng. Chem. Res. 35 (1996) 1383.
[23] R. Prasad, K.K. Sirkar, Dispersion-free solvent extraction with microporous hollow fiber modules, AIChE J. 34 (1988) 177.
[24] A.B. Haan, P.V. Bartels, J. Graauw, Extraction of metal ions from waste water. Modeling of the mass transfer in a supported liquid membrane process, J. Membr. Sci. 45 (1989) 281.
[25] L. Dahuron, E.L. Cussler, Protein extractions with hollow fibers, AIChE J. 34 (1) (1988) 130.
[26] (a) X. Lévêque, Les lois de la transmission de chaleur par conduction, Ann. Mines 13 (1928) 201;
(b) L. Graetz, Uber die Warmeletungsfahigkeit von Flussigkeiten, Ann. Phys. Chem. 18 (1883) 79;
(c) L. Graetz, Uber die Warmeletungsfahigkeit von Flussigkeiten, Ann. Phys. Chem. 25 (1885) 337;
(d) J.G. Knudsen, D.L. Katz, Fluid dynamics and heat transfer, McGraw-Hill, New York, 1958;
(e) B.W. Reed, M.J. Semmens, E.L. Cussler, Membrane contactors, in: R.D. Noble, S.A. Stern (Eds.), Membrane Separation Technology, Principles and Applications, Elsevier, Amsterdam, 1995, p. 474.;
(f) S.R. Wickramasinghe, M.J. Semmens, E.L. Cussler, Mass transfer in various hollow fiber geometries, J. Membr. Sci. 69 (1992) 235–250;
(g) J.K. Park, H.N. Chang, Flow distribution in the lumen side of a hollow fiber module, AIChE J. 32 (1986) 1937–1947.
[27] R. Basu, R. Prasad, K.K. Sirkar, Non-dispersive membrane solvent back extraction of phenol, AIChE J. 36 (1990) 450.
[28] A. Kiani, R.R. Bhave, K.K. Sirkar, Solvent extraction with immobilised interfaces in a microporous hydrophobic membrane, J. Membr. Sci. 20 (1984) 125.
[29] R. Prasad, A. Kiani, R.R. Bhave, K.K. Sirkar, Further studies on solvent extraction with immobilized interfaces in a microporous hydrophobic membrane, J. Membr. Sci. 26 (1986) 79.
[30] S.B. Iversion, V.K. Bhatia, K. Dam-Johansen, G. Jonsson, Characterisation of microporous membranes for use in membrane contactors, in: Proceedings of the Seventh International Symposium on Synthetic Membranes in Science and Industry, Decchema e.v., Frankfurt am Main, Germany, 1994, pp. 22–23.
[31] P.R. Alexander, R.W. Callahan, Liquid–liquid extraction and stripping of gold with microporous hollow fibers, J. Membr. Sci. 35 (1987) 57.
[32] A.K. Pabby, A.M. Sastre, Hollow fiber membrane based separation technology: performance and design perspectives, in: Cortina, Aguilar (Eds.), Solvent Extraction and Liquid Membranes: Fundamental and Application in New Materials, Marcel Dekker, New York, in press.
[33] R. Prasad, K.K. Sirkar, Hollow fiber solvent extraction: performances and design, J. Membr. Sci. 50 (1990) 153–175.
[34] S.R. Wickramasinghe, M.J. Semmens, E.L. Cussler, Mass transfer in various hollow fiber geometries, J. Membr. Sci. 69 (1992) 235–250.
[35] M.J. Costello, A.G. Fane, P.G. Hogan, R.W. Schofield, The effect of shell side hydrodynamics on the performance of axial flow hollow fiber modules, J. Membr. Sci. 80 (1993) 11.
[36] J.D. Rogers, R.L. Long Jr., Modeling hollow fiber membrane contactors film theory, Voronoi tessellations, and facilitation factors for systems with interface reactions, J. Membr. Sci. 134 (1997) 1–17.